

Proton- ^3H scattering calculation: Elastic and charge-exchange reactions up to 30 MeV

A. Deltuva

Institute of Theoretical Physics and Astronomy, Vilnius University, A. Goštauto 12, LT-01108 Vilnius, Lithuania

A. C. Fonseca

Centro de Física Nuclear da Universidade de Lisboa, P-1649-003 Lisboa, Portugal

(Received July 13, 2018)

Proton- ^3H elastic scattering and charge-exchange reaction $^3\text{H}(p, n)^3\text{He}$ in the energy regime above four-nucleon breakup threshold are described in the momentum-space transition operator framework. Fully converged results are obtained using realistic two-nucleon potentials and two-proton Coulomb force as dynamic input. Differential cross section, proton analyzing power, outgoing neutron polarization, and proton-to-neutron polarization transfer coefficients are calculated between 6 and 30 MeV proton beam energy. Good agreement with the experimental data is found for the differential cross section both in elastic and charge-exchange reactions; the latter shows a complicated energy and angular dependence. The most sizable discrepancies between predictions and data are found for the proton analyzing power and outgoing neutron polarization in the charge-exchange reaction, while the respective proton-to-neutron polarization transfer coefficients are well described by the calculations.

PACS numbers: 21.45.-v, 21.30.-x, 25.10.+s, 24.70.+s

I. INTRODUCTION

The theoretical understanding of the structure of nuclei along the valley of stability, as well as away from it up to the neutron or proton drip lines, has advanced fast in the last 15 years through state-of-the-art microscopic Green's function Monte Carlo (GFMC) [1, 2] and No Core Shell Model (NCSM) [3] calculations based on realistic nucleon-nucleon (NN) and three-nucleon ($3N$) force models. In contrast, the corresponding advances in the study of nuclear reactions have been meager and mostly limited to the three- and four-nucleon ($4N$) systems. As discussed in a recent review article [4], this may change in the near future as one implements algorithms capable of applying bound state techniques to the solution of the multiparticle scattering problem. Until this becomes a reliable pathway, one follows the traditional approach by solving coordinate- or momentum-space equations with appropriate boundary conditions that are equivalent to solving the corresponding n -particle Schrödinger equation.

Although rigorous n -particle scattering equations were derived almost 50 years ago by Faddeev and Yakubovsky (FY) [5, 6] and by Alt, Grassberger, and Sandhas (AGS) [7, 8], exact numerical solutions of the $3N$ and $4N$ scattering problems only became possible with the advent of fast and larger computers, together with powerful numerical techniques such as spline interpolation, Padé summation, and many others. Neutron-deuteron (n - d) scattering calculations with realistic NN force models reached state-of-the-art status in the early 1990's due to the effort of a number of independent groups [9–13]. Owing to the difficulties in treating the long-range Coulomb force, fully converged proton-deuteron (p - d) scattering calculations came later [14–17]. Due to its higher dimensionality and

multichannel complexity, the $4N$ scattering problem took twenty years longer to reach the same status as the $3N$ system except for the calculation of breakup reactions. There have been also attempts to calculate scattering processes involving five and more nucleons but using different methods than in the $3N$ and $4N$ systems, namely, GFMC [18] and the NCSM resonating group [19].

Although the $4N$ system has a long history that started out in the early 1970's [20], most of the recent developments are mainly due to the works of the Pisa [21–24], Grenoble-Strasbourg [25–28], and Lisbon [29–32] groups. Because the first two groups use the coordinate-space representation, they were able to include not only realistic NN interactions but also $3N$ forces. Nevertheless, they have had a major difficulty in calculating multichannel reactions and going beyond breakup threshold, particularly when the Coulomb interaction between protons is included. The Lisbon group uses the momentum-space AGS equations for transition operators [8] that were solved for multichannel reactions both below [33] and above [34] breakup threshold and with the Coulomb force included. The only stumbling block has been the inclusion of irreducible $3N$ forces. For this reason we are not yet able to perform calculations with NN and $3N$ potentials derived from the chiral effective field theory; only the NN part has been included in our calculations [29, 33]. An alternative is a nuclear force model with explicit excitation of a nucleon to a Δ isobar. This coupling generates both effective $3N$ and $4N$ forces that have been successfully included in $4N$ calculations by the Lisbon-Hannover collaboration [35].

In the past two years we produced a realm of results for cross sections and polarizations observables for the elastic scattering of a neutron (n) on a ^3H target [31] and a proton (p) on a ^3He target [32] above the breakup

threshold. These processes are dominated by the total isospin $\mathcal{T} = 1$ states. More recently we presented results for the mixed isospin ($\mathcal{T} = 0$ and 1) processes initiated by the $n + {}^3\text{He}$ collisions [36] that are coupled multichannel reactions leading to all energetically allowed final states $n + {}^3\text{He}$, $p + {}^3\text{H}$, $d + d$, $d + n + p$, and $n + n + p + p$.

In the present work we study in detail the $p + {}^3\text{H}$ scattering above the breakup threshold. We concentrate on elastic and charge-exchange reactions for which there is abundant experimental data, but also some inconsistencies between different data sets, that might be sorted out through accurate theoretical predictions. These calculations are especially important given that novel experiments are hardly possible due to the lack of ${}^3\text{H}$ targets or proper facilities that still operate at these energies. Furthermore, new $4N$ scattering calculations are also worth pursuing because they lead the way to the solution of complicated multiparticle scattering problems, not just in nuclear physics but also in cold atom physics [37], and in the study of complex nuclear reactions that exhibit two-body degrees of freedom such as the scattering of a two-neutron halo nucleus on a proton target.

In Sec. II we shortly recall the theoretical formalism and in Sec. III we present the numerical results. The summary is given in Sec. IV.

II. 4N SCATTERING EQUATIONS

We employ the isospin formalism for the description of the $4N$ scattering. Since $p + {}^3\text{H}$ is the mirror of the $n + {}^3\text{He}$ system, we take over the calculational technique from Ref. [36] where $4N$ reactions initiated by the $n + {}^3\text{He}$ collisions were described. Thus, we use the momentum-space partial-wave framework to solve the integral AGS equations [8] for symmetrized four-particle transition operators

$$\mathcal{U}_{11} = -(G_0 t G_0)^{-1} P_{34} - P_{34} U_1 G_0 t G_0 \mathcal{U}_{11} + U_2 G_0 t G_0 \mathcal{U}_{21}, \quad (1a)$$

$$\mathcal{U}_{21} = (G_0 t G_0)^{-1} (1 - P_{34}) + (1 - P_{34}) U_1 G_0 t G_0 \mathcal{U}_{11}. \quad (1b)$$

Here $G_0 = (E + i\varepsilon - H_0)^{-1}$ is the free resolvent with the complex energy $E + i\varepsilon$ and the free Hamiltonian H_0 , t is the NN transition matrix, P_{ab} is the permutation operator of particles a and b , and U_α are the transition operators for the 3+1 ($\alpha = 1$) and 2+2 ($\alpha = 2$) subsystems. The on-shell matrix elements of the operators $\mathcal{U}_{\beta\alpha}$ taken at $\varepsilon \rightarrow +0$ yield the transition amplitudes for two-cluster reactions. In the isospin formalism the NN transition matrix has contributions from nn , np , and pp pairs with the respective weights given in Ref. [36]; for the pp pair the screened Coulomb interaction is included and the resulting physical amplitudes for $4N$ reactions are obtained by using the method of screening and renormalization [16, 33, 38, 39]. Further explanations and technical details can be found in Refs. [34, 36].

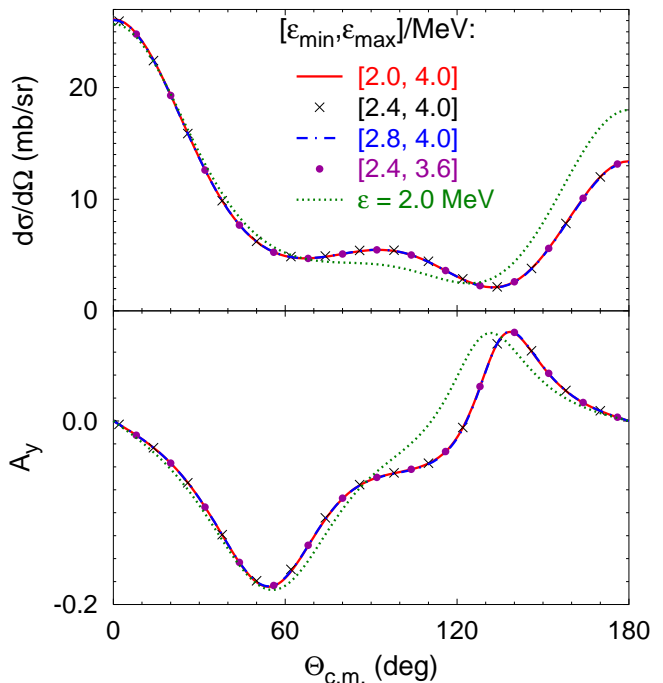


FIG. 1. (Color online) Differential cross section and proton analyzing power for ${}^3\text{H}(p,n){}^3\text{He}$ reaction at 24 MeV proton energy as functions of the c.m. scattering angle. Results obtained using different sets of ε values ranging from ε_{\min} to ε_{\max} with the step of 0.4 MeV are compared; they are indistinguishable. The dotted curves refer to the $\varepsilon = 2.0$ MeV calculations without extrapolation that have no physical meaning but show the importance of the extrapolation.

To avoid the very complicated singularity structure of the kernel, we solve Eqs. (1) numerically at several complex energies $E + i\varepsilon_j$ with finite values of $\varepsilon_j > 0$ and then extrapolate the obtained on-shell matrix elements of the transition operators $\mathcal{U}_{\beta\alpha}$ to the $\varepsilon \rightarrow +0$ limit which corresponds to the physical scattering process; more details are given in Ref. [31] using $n + {}^3\text{H}$ elastic scattering as an example. In Fig. 1 we demonstrate that the employed method is accurate and reliable also for inelastic reactions. As an example we consider the charge-exchange reaction ${}^3\text{H}(p,n){}^3\text{He}$ at 24 MeV proton energy. The transition amplitudes were calculated at six values of $\varepsilon_j > 0$ ranging from 2 to 4 MeV, and then extrapolated to the $\varepsilon \rightarrow +0$ limit using four different sets. In all four cases the resulting differential cross section and proton analyzing power turn out to be indistinguishable in the plot, whereas the predictions at finite $\varepsilon = 2$ MeV without extrapolation deviate significantly.

III. RESULTS

We consider $p + {}^3\text{H}$ scattering at proton energies E_p ranging from 6 to 30 MeV; the regime below 6 MeV was studied by us in Ref. [33]. Most results are ob-

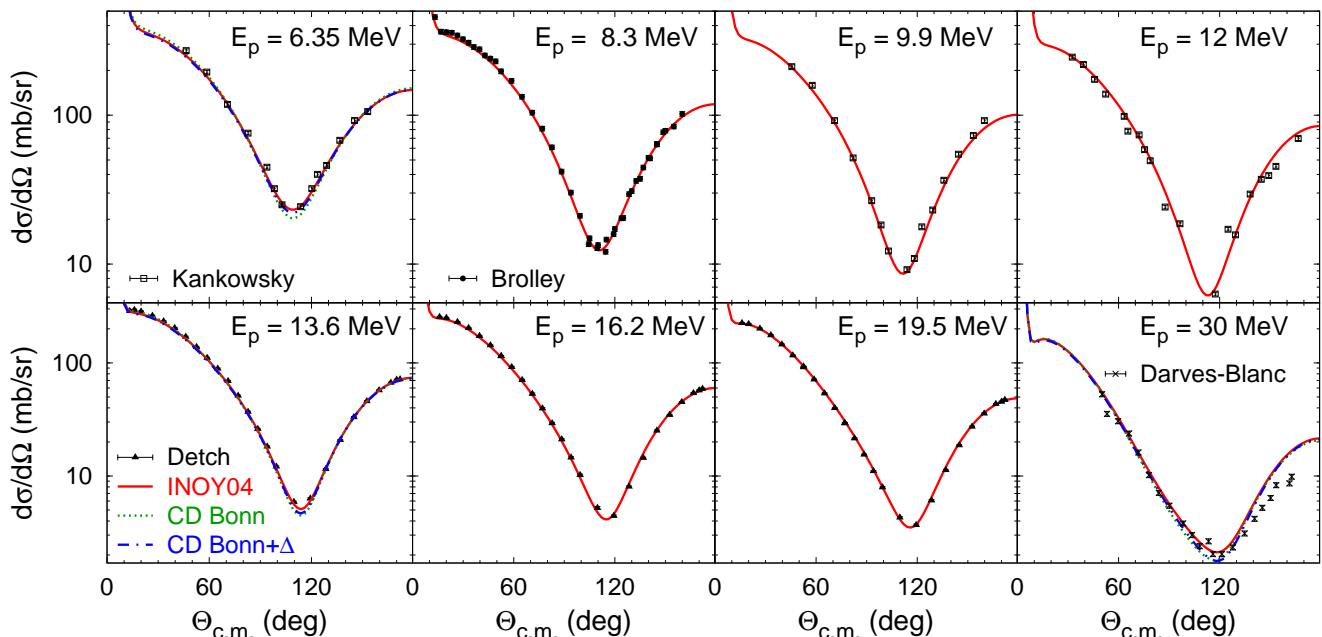


FIG. 2. (Color online) Differential cross section of elastic $p + {}^3\text{H}$ scattering at proton energy between 6.35 and 30 MeV. Results obtained with potentials INOY04 (solid curves), CD Bonn (dotted curves), and CD Bonn + Δ (dashed-dotted curves) are compared with data from Refs. [40–43].

tained using the realistic inside-nonlocal outside-Yukawa (INOY04) potential by Doleschall [26, 44]. It predicts the ${}^3\text{He}$ (${}^3\text{H}$) binding energy to be 7.73 MeV (8.49 MeV) and thereby nearly reproduces the experimental value of 7.72 MeV (8.48 MeV) without an additional $3N$ force. To investigate the dependence of our results on the interaction model, at several energies we also show the predictions obtained with other high-precision NN potentials, namely, the charge-dependent Bonn potential (CD Bonn) [45] and its extension CD Bonn + Δ [46] explicitly including an excitation of a nucleon to a Δ isobar. This mechanism generates effective $3N$ and $4N$ forces that are mutually consistent but quantitatively still insufficient to reproduce $3N$ and $4N$ binding energies, although they reduce the discrepancy [35]. For ${}^3\text{He}$ and ${}^3\text{H}$ binding energies the CD Bonn + Δ potential yields 7.53 and 8.28 MeV, while the predictions of CD Bonn are 7.26 and 8.00 MeV, respectively. In addition to INOY04, results for CD Bonn + Δ are presented at $E_p = 6.0, 6.35, 13.6,$ and 30.0 MeV while for CD Bonn at $E_p = 6.0, 6.35, 7.0, 9.0, 13.0, 13.6, 21.0,$ and 30.0 MeV.

In Fig. 2 we show the differential cross section $d\sigma/d\Omega$ for elastic $p + {}^3\text{H}$ scattering as a function of the center of mass (c.m.) scattering angle $\Theta_{\text{c.m.}}$. This observable decreases with the increasing energy while its minimum moves slowly to higher angles; the INOY04 calculations describe the energy and angular dependence of the experimental data [40, 42, 43, 47] fairly well except at backward angles at 30 MeV. However, one may question the reliability of those data [43] that exhibit quite

an abrupt decrease from $E_p = 19.5$ MeV to $E_p = 30$ MeV while other data and theoretical predictions vary smoothly with energy. Unfortunately, we found no data between $E_p = 20$ and 30 MeV that would help sort out this possible discrepancy. The sensitivity to the force model manifests itself in the minimum where predictions obtained with CD Bonn and CD Bonn + Δ are below those of INOY04 by about 15 %.

It is interesting to compare the present $p + {}^3\text{H}$ results with those for $n + {}^3\text{H}$ [31], $p + {}^3\text{He}$ [32], and $n + {}^3\text{He}$ [36] elastic scattering. Since the energy and force model dependence for $p + {}^3\text{H}$ and $n + {}^3\text{He}$ calculations are the same as can be expected from the isospin symmetry, one would expect similar discrepancies between data and theory assuming that the data can be equally trusted. However, the agreement with the experimental data is different in these two cases. We note that for $p + {}^3\text{H}$ there is no discrepancy at the minimum of the differential cross section as the proton energy increases towards 30 MeV, while in $n + {}^3\text{He}$ and $p + {}^3\text{He}$ elastic scattering the minimum is underpredicted by the theoretical calculations as the energy of the incoming beam rises above 25 MeV. In contrast, the $n + {}^3\text{H}$ data, only available at 22 MeV, are overpredicted [31].

In Fig. 3 we show the proton analyzing power A_y for the elastic $p + {}^3\text{H}$ scattering at proton energies ranging from 6.35 to 30 MeV. The qualitative reproduction of the experimental data by our calculations is reasonable. The existing discrepancies around the minimum and the maximum decrease as the energy increases reaching a good

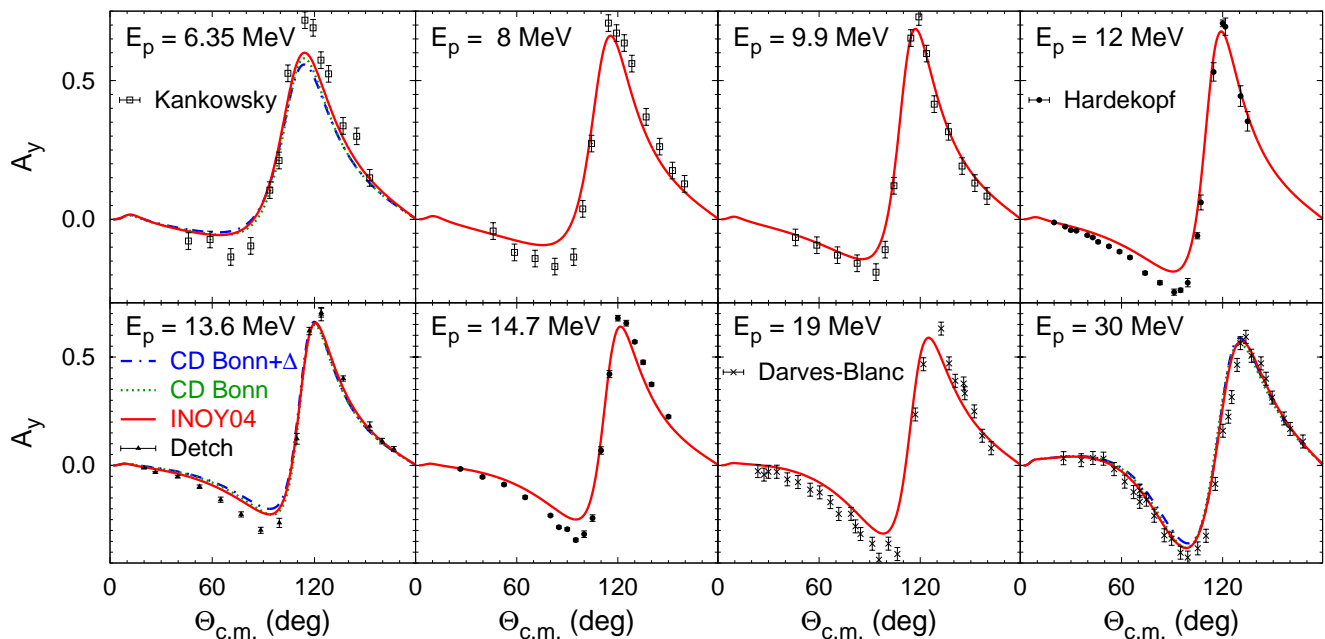


FIG. 3. (Color online) Proton analyzing power of elastic $p + {}^3\text{H}$ scattering at proton energy between 6.35 and 30 MeV. Curves are as in Fig. 2. Data are from Refs. [40, 42, 43, 47].

agreement at $E_p = 30$ MeV. The sensitivity to the nuclear force model is quite weak. In all these respects the behavior of the A_y in the elastic $p + {}^3\text{H}$ scattering is qualitatively the same as observed for the neutron analyzing power in the $n + {}^3\text{He}$ elastic scattering [36].

Next we consider rearrangement reactions initiated by $p + {}^3\text{H}$ collisions. In Fig. 4 we show the differential cross section $d\sigma/d\Omega$ for the charge exchange reaction ${}^3\text{H}(p, n){}^3\text{He}$ at E_p ranging from 6 to 30 MeV. The data [48–51] exhibits a strong energy dependency that is well reproduced by the theoretical calculations, in particular the shape of the observable that starts out backward peaked at 6 MeV with a single shallow minimum around 90° , and ends up forward peaked at 30 MeV with two minima around 60° and 140° . The appearance of a local maximum and two local minima in both theory and data takes place at $E_p = 9$ MeV. Predictions of the three employed force models follow the same trend but in particular regimes may differ by almost 20 % as happens at $E_p = 13.6$ MeV and $\Theta_{\text{c.m.}} = 0^\circ$. At lower energies the sensitivity to the NN potential shows up at forward and backward angles while above 20 MeV it extends to the whole angular regime, being around 10 %. The effect seems to be more complicated than just a simple scaling with $3N$ binding energy since the predictions of CD Bonn and CD Bonn + Δ stay quite close together but deviate more from INOY04. While at lower energies the INOY04 potential is favored by the data, above 20 MeV the best description is provided by the CD Bonn potential whereas INOY04 overpredicts the data. In addition, there are also some inconsistencies between different data

sets, e.g., the first few points from Ref. [51] seem to be wrong when compared to other measurements [48–50].

Unlike the differential cross section, the proton analyzing power A_y and the outgoing neutron polarization P_y for the charge-exchange reaction ${}^3\text{H}(p, n){}^3\text{He}$ displayed in Fig. 5 show a large quantitative disagreement between theoretical results and experimental data, especially at the lowest considered energy $E_p = 6$ MeV. Here the predicted shape of these observables is roughly correct but the absolute value is too small by a factor of 2. The disagreement decreases with increasing energy but for A_y still remains about 25 % at $E_p = 13.6$ MeV, the highest energy where data are available. Thus, nucleon vector polarization observables A_y and P_y in the charge-exchange reaction ${}^3\text{H}(p, n){}^3\text{He}$ exhibit one of the largest discrepancies seen so far in the $4N$ system. The sensitivity to the force model is significant only at the lowest energy where, in contrary to what can be expected from scaling with $3N$ binding energy, the discrepancy is largest for INOY04 and smallest for CD Bonn. This sensitivity as well as the very strong energy dependence of A_y observed in Ref. [33] might be due to the interplay of P -wave $4N$ resonant states existing at low energies. Away from this resonant regime the observables become less sensitive, and at $E_p = 13.6$ MeV the predictions of INOY04 are slightly closer to the data than those of other potentials. The A_y and P_y discrepancies observed in the ${}^3\text{H}(p, n){}^3\text{He}$ reaction may be one more manifestation of the famous A_y puzzle seen in the elastic nucleon-deuteron and nucleon-trinucleon scattering [12, 14, 21, 24, 30, 32]. However, there is also an important difference: the cor-

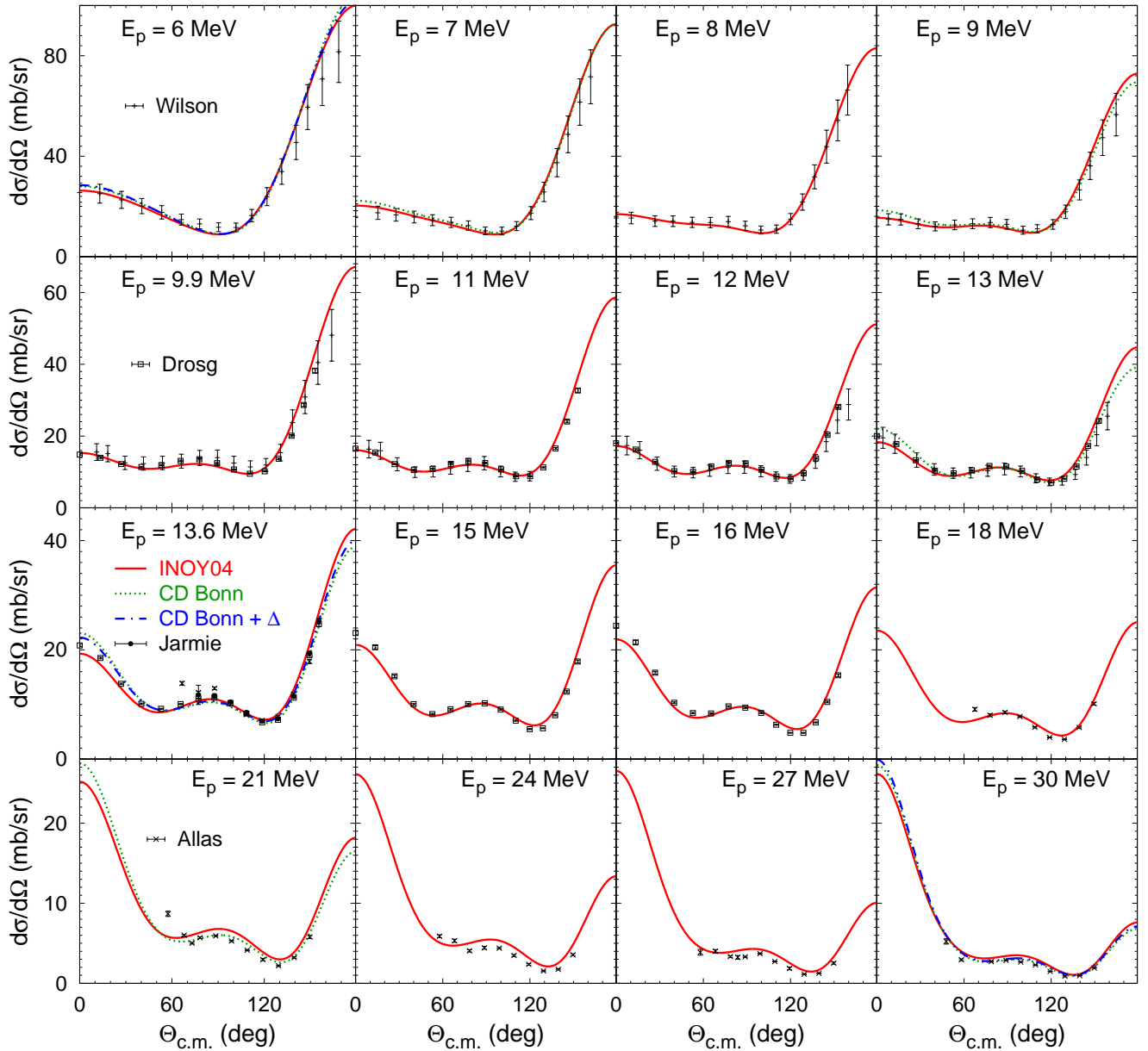


FIG. 4. (Color online) Differential cross section of ${}^3\text{H}(p, n){}^3\text{He}$ reaction. Curves are as in Fig. 2. Data are from Refs. [48–51].

relation between the discrepancy and the predicted $3N$ binding energy in the charge-exchange reaction below 10 MeV gets reversed as compared to all elastic processes. For example, the INOY04 potential shows the smallest discrepancy in the elastic scattering but the largest one in the ${}^3\text{H}(p, n){}^3\text{He}$ reaction.

Although "two wrongs do not necessarily make one right", the proton-to-neutron polarization (spin) transfer coefficients $K_x^{x'}$, $K_z^{x'}$, and K_y^y for the charge-exchange reaction ${}^3\text{H}(p, n){}^3\text{He}$ at $E_p = 6.0, 9.9,$ and 13.6 MeV presented in Fig. 6 are well reproduced by the theoretical calculations. The spin transfer coefficients show rather com-

plicated angular and energy dependence which is non-monotonic as can be seen most clearly in $K_x^{x'}$ and K_y^y at small angles. The sensitivity of these observables to the choice of the NN force model is moderate over the whole considered energy and angular regime. It is not unusual in few-nucleon physics that double-polarization observables such as spin correlation or spin transfer coefficients are in better agreement with the experimental data than analyzing powers; $p + {}^3\text{He}$ elastic scattering [30, 32] is a further example. Unfortunately, double-polarization data are missing in $n + {}^3\text{He}$ and $p + {}^3\text{H}$ elastic scattering.

Regarding the transfer reaction ${}^3\text{H}(p, d){}^2\text{H}$, first results for the differential cross section at $E_p = 13.6$ MeV

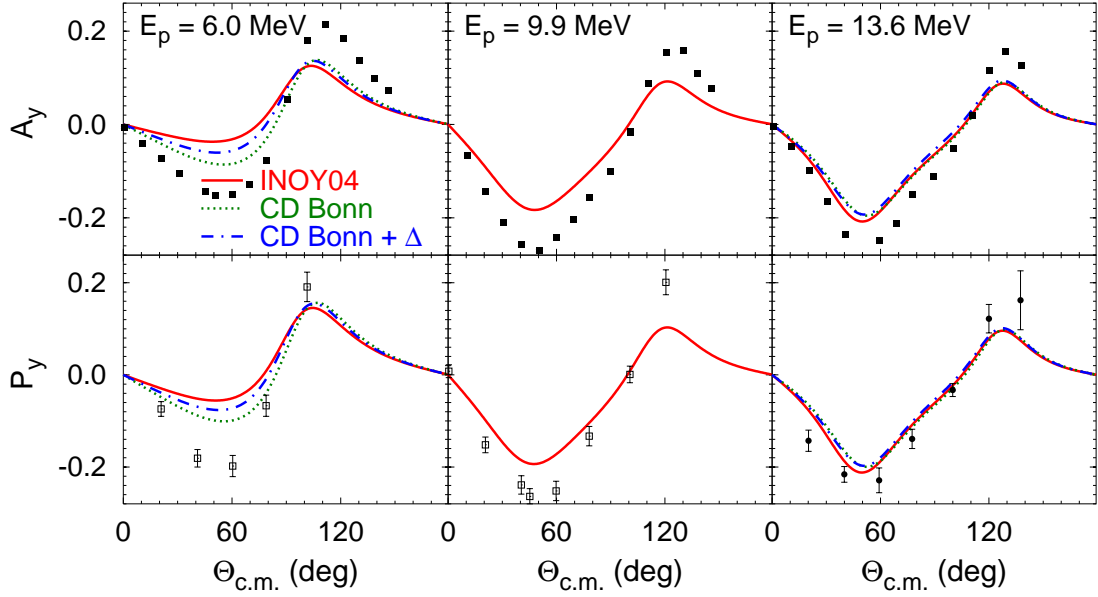


FIG. 5. (Color online) Proton analyzing power A_y and outgoing neutron polarization P_y in the ${}^3\text{H}(p,n){}^3\text{He}$ reaction at 6.0, 9.9, and 13.6 MeV proton energy. Curves are as in Fig. 2. The data are from Ref. [52] for A_y and from Refs. [53] (\square) and [54] (\bullet) for P_y .

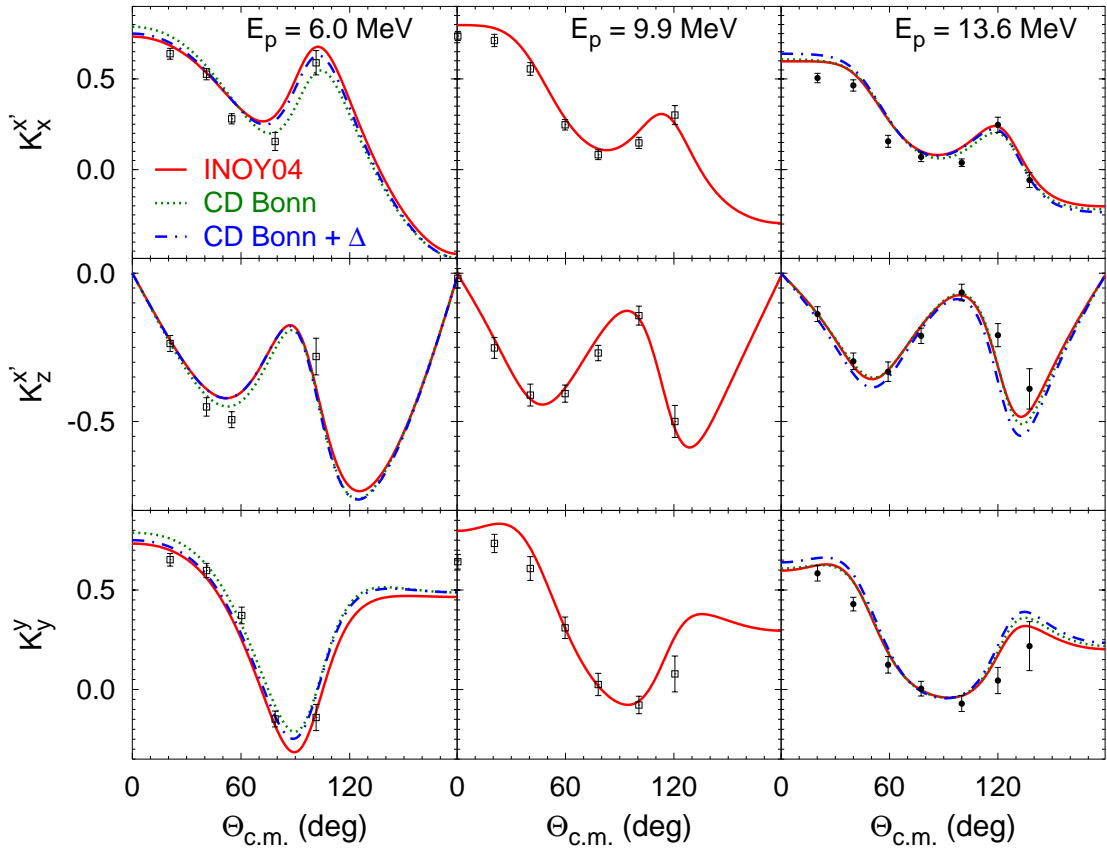


FIG. 6. (Color online) Proton-to-neutron polarization transfer coefficients of ${}^3\text{H}(p,n){}^3\text{He}$ reaction at 6.0, 9.9, and 13.6 MeV proton energy. Curves are as in Fig. 2. The data are from Refs. [53] (\square) and [54] (\bullet).

were presented in Ref. [34]; quite a good agreement between predictions and data was found with only slight underestimation around $\Theta_{\text{c.m.}} = 90^\circ$. Since the experimental studies of nucleon transfer processes in the $4N$ system have been dominated by the time reversed reaction ${}^2\text{H}(d,p){}^3\text{H}$ and its mirror partner ${}^2\text{H}(d,n){}^3\text{He}$, their theoretical analysis will be presented in the forthcoming work on the $d+d$ scattering [55].

IV. SUMMARY

In this work we studied $p + {}^3\text{H}$ elastic scattering and the charge-exchange reaction ${}^3\text{H}(p,n){}^3\text{He}$ up to 30 MeV beam energy. We solved, in a numerically converged way, the momentum-space Alt, Grassberger, and Sandhas equations for transition operators. The employed complex-energy method with special integration weights proved to be highly reliable also for inelastic reactions such as ${}^3\text{H}(p,n){}^3\text{He}$. The calculations include the Coulomb interaction between protons together with realistic NN force models, i.e., INOY04, CD Bonn, and CD Bonn + Δ . An explicit excitation of a nucleon to a Δ isobar included in the latter model yields mutually consistent effective $3N$ and $4N$ forces. Moderate sensitivity to the employed interaction model is found in several observables in particular energy regimes, most of them referring to the ${}^3\text{H}(p,n){}^3\text{He}$ reaction. Like the previous work on $n + {}^3\text{H}$, $p + {}^3\text{He}$, and $n + {}^3\text{He}$ scattering [31, 32, 34, 36], this is a state-of-the-art calculation that shows the virtues and limitations of realistic NN force models in describing the world data up to 30 MeV beam

energy for elastic and charge-exchange reactions initiated by $p + {}^3\text{H}$ collisions. We find that elastic and charge-exchange differential cross sections are well described by the calculations in the considered energy regime between 6 and 30 MeV. The absence of a discrepancy in the minimum of the elastic differential cross section at 30 MeV is quite surprising given that such discrepancies show up in $p + {}^3\text{He}$ and $n + {}^3\text{He}$ elastic scattering. In the ${}^3\text{H}(p,n){}^3\text{He}$ case the predicted differential cross section varies very rapidly with the energy, developing new local minima and maxima in the angular distribution that are seen also in the experimental data. The elastic proton analyzing power A_y is fairly well described by the calculations showing the usual discrepancies in the minima and maxima already observed in other elastic $4N$ collisions driven by proton or neutron beams. The largest discrepancies between data and calculations are observed in the proton analyzing power A_y and outgoing neutron polarization P_y in the charge-exchange reaction ${}^3\text{H}(p,n){}^3\text{He}$. In contrast, proton-to-neutron polarization transfer coefficients in the charge-exchange reaction are successfully described by theory in spite of their complex structure and variation with beam energy. This and previous achievements show that, after many years of hard work, numerically converged solutions of the $4N$ scattering problem with realistic NN force models are not only possible but also that such endeavor has reached a level of sophistication and reliability only comparable to $3N$ scattering studies. Nevertheless, much remains to be done, such as calculating breakup observables or including irreducible $3N$ forces in momentum-space calculations. Progress in this direction is forthcoming.

-
- [1] S. C. Pieper, V. R. Pandharipande, R. B. Wiringa, and J. Carlson, *Phys. Rev. C* **64**, 014001 (2001).
- [2] S. C. Pieper, K. Varga, and R. B. Wiringa, *Phys. Rev. C* **66**, 044310 (2002).
- [3] E. Caurier, P. Navrátil, W. E. Ormand, and J. P. Vary, *Phys. Rev. C* **66**, 024314 (2002).
- [4] J. Carbonell, A. Deltuva, A. Fonseca, and R. Lazauskas, *Progress in Particle and Nuclear Physics* **74**, 55 (2014).
- [5] L. D. Faddeev, *Zh. Eksp. Teor. Fiz.* **39**, 1459 (1960) [*Sov. Phys. JETP* **12**, 1014 (1961)].
- [6] O. A. Yakubovsky, *Yad. Fiz.* **5**, 1312 (1967) [*Sov. J. Nucl. Phys.* **5**, 937 (1967)].
- [7] E. O. Alt, P. Grassberger, and W. Sandhas, *Nucl. Phys.* **B2**, 167 (1967).
- [8] P. Grassberger and W. Sandhas, *Nucl. Phys.* **B2**, 181 (1967); E. O. Alt, P. Grassberger, and W. Sandhas, JINR report No. E4-6688 (1972).
- [9] Y. Koike and Y. Taniguchi, *Few-Body Systems* **1**, 13 (1986).
- [10] C. R. Chen, G. L. Payne, J. L. Friar, and B. F. Gibson, *Phys. Rev. C* **39**, 1261 (1989).
- [11] J. L. Friar *et al.*, *Phys. Rev. C* **42**, 1838 (1990).
- [12] T. Cornelius, W. Glöckle, J. Haidenbauer, Y. Koike, W. Plessas, and H. Witała, *Phys. Rev. C* **41**, 2538 (1990).
- [13] A. Kievsky, S. Rosati, W. Tornow, and M. Viviani, *Nucl. Phys.* **A607**, 402 (1996).
- [14] A. Kievsky, M. Viviani, and S. Rosati, *Phys. Rev. C* **64**, 024002 (2001).
- [15] C. R. Chen, J. L. Friar, and G. L. Payne, *Few-Body Syst.* **31**, 13 (2001).
- [16] A. Deltuva, A. C. Fonseca, and P. U. Sauer, *Phys. Rev. C* **71**, 054005 (2005).
- [17] A. Deltuva, A. C. Fonseca, and P. U. Sauer, *Phys. Rev. C* **72**, 054004 (2005).
- [18] K. M. Nollett, S. C. Pieper, R. B. Wiringa, J. Carlson, and G. M. Hale, *Phys. Rev. Lett.* **99**, 022502 (2007).
- [19] S. Quaglioni and P. Navratil, *Phys. Rev. Lett.* **101**, 092501 (2008).
- [20] A. C. Fonseca, in *Lecture Notes in Physics 273* (Springer, Heidelberg, 1987), p. 161.
- [21] M. Viviani, A. Kievsky, S. Rosati, E. A. George, and L. D. Knutson, *Phys. Rev. Lett.* **86**, 3739 (2001).
- [22] A. Kievsky, S. Rosati, M. Viviani, L. E. Marcucci, and L. Girlanda, *J. Phys. G* **35**, 063101 (2008).
- [23] M. Viviani, R. Schiavilla, L. Girlanda, A. Kievsky, and L. E. Marcucci, *Phys. Rev. C* **82**, 044001 (2010).
- [24] M. Viviani, L. Girlanda, A. Kievsky, and L. E. Marcucci, *Phys. Rev. Lett.* **111**, 172302 (2013).

- [25] R. Lazauskas, Ph.D. thesis, Université Joseph Fourier, Grenoble, 2003, <http://tel.ccsd.cnrs.fr/documents/archives0/00/00/41/78/>.
- [26] R. Lazauskas and J. Carbonell, *Phys. Rev. C* **70**, 044002 (2004).
- [27] R. Lazauskas, *Phys. Rev. C* **79**, 054007 (2009).
- [28] R. Lazauskas, *Phys. Rev. C* **86**, 044002 (2012).
- [29] A. Deltuva and A. C. Fonseca, *Phys. Rev. C* **75**, 014005 (2007).
- [30] A. Deltuva and A. C. Fonseca, *Phys. Rev. Lett.* **98**, 162502 (2007).
- [31] A. Deltuva and A. C. Fonseca, *Phys. Rev. C* **86**, 011001(R) (2012).
- [32] A. Deltuva and A. C. Fonseca, *Phys. Rev. C* **87**, 054002 (2013).
- [33] A. Deltuva and A. C. Fonseca, *Phys. Rev. C* **76**, 021001(R) (2007).
- [34] A. Deltuva and A. C. Fonseca, *Phys. Rev. Lett.* **113**, 102502 (2014).
- [35] A. Deltuva, A. C. Fonseca, and P. U. Sauer, *Phys. Lett. B* **660**, 471 (2008).
- [36] A. Deltuva and A. C. Fonseca, *Phys. Rev. C* **90**, 044002 (2014).
- [37] A. Deltuva, *Phys. Rev. A* **82**, 040701(R) (2010).
- [38] J. R. Taylor, *Nuovo Cimento B* **23**, 313 (1974); M. D. Semon and J. R. Taylor, *Nuovo Cimento A* **26**, 48 (1975).
- [39] E. O. Alt and W. Sandhas, *Phys. Rev. C* **21**, 1733 (1980).
- [40] R. Kankowsky, J. C. Fritz, K. Kilian, A. Neufert, and D. Fick, *Nucl. Phys.* **A263**, 29 (1976).
- [41] J. E. Brolley, T. M. Putnam, L. Rosen, and L. Stewart, *Phys. Rev.* **117**, 1307 (1960).
- [42] J. L. Detch, R. L. Hutson, N. Jarmie, and J. H. Jett, *Phys. Rev. C* **4**, 52 (1971).
- [43] R. Darves-Blanc, N. Sen, J. Arvieux, A. Fiore, J. Gondrand, and G. Perrin, *Lett. Nuovo Cimento* **4**, 16 (1972).
- [44] P. Doleschall, *Phys. Rev. C* **69**, 054001 (2004).
- [45] R. Machleidt, *Phys. Rev. C* **63**, 024001 (2001).
- [46] A. Deltuva, R. Machleidt, and P. U. Sauer, *Phys. Rev. C* **68**, 024005 (2003).
- [47] R. Hardekopf, P. Lisowski, T. Rhea, R. Walter, and T. Clegg, *Nucl. Phys. A* **191**, 481 (1972).
- [48] W. E. Wilson, R. L. Walter, and D. B. Fossan, *Nucl. Phys.* **27**, 421 (1961).
- [49] M. Drog, *Nucl. Sci. Eng.* **67**, 190 (1978); in EXFOR Database (NNDC, Brookhaven, 1978).
- [50] N. Jarmie and J. H. Jett, *Phys. Rev. C* **16**, 15 (1977).
- [51] R. G. Allas, L. A. Beach, R. O. Bondelid, E. M. Diener, E. L. Petersen, J. M. Lambert, P. A. Treado, and I. Slaus, *Phys. Rev. C* **9**, 787 (1974).
- [52] J. J. Jarmer, R. C. Haight, J. E. Simmons, J. C. Martin, and T. R. Donoghue, *Phys. Rev. C* **9**, 1292 (1974).
- [53] J. J. Jarmer, R. C. Haight, J. C. Martin, and J. E. Simmons, *Phys. Rev. C* **10**, 494 (1974).
- [54] R. C. Haight, J. E. Simmons, and T. R. Donoghue, *Phys. Rev. C* **5**, 1826 (1972).
- [55] A. Deltuva and A. C. Fonseca, *Phys. Lett. B*, submitted.